Effect of a ketogenic diet on hepatic steatosis and hepatic mitochondrial metabolism in nonalcoholic fatty liver disease

Panu K. Luukkonen[a,b,c], Sylvie Dufour[a,d], Kun Lyu[e], Xian-Man Zhang[a,d], Antti Hakkarainen[f,g], Tiina E. Lehtimäki[f], Gary W. Cline[a,d], Kitt Falk Petersen[a,d], Gerald I. Shulman[a,d,e,1,2], and Hannele Yki-Järvinen[b,c,1,2]

[a]Department of Internal Medicine, Yale School of Medicine, New Haven, CT 06520; [b]Minerva Foundation Institute for Medical Research, Helsinki 00290, Finland; [c]Department of Medicine, University of Helsinki and Helsinki University Hospital, Helsinki 00290, Finland; [d]Yale Diabetes Research Center, Yale School of Medicine, New Haven, CT 06520; [e]Department of Cellular & Molecular Physiology, Yale School of Medicine, New Haven, CT 06520; [f]Department of Radiology, HUS Medical Imaging Center, University of Helsinki and Helsinki University Hospital, Helsinki 00290, Finland; and [g]Department of Neuroscience and Biomedical Engineering, Aalto University School of Science, 00076 Espoo, Finland

Contributed by Gerald I. Shulman, January 31, 2020 (sent for review December 26, 2019; reviewed by Fredrik Karpe and Roy Taylor)

Weight loss by ketogenic diet (KD) has gained popularity in management of nonalcoholic fatty liver disease (NAFLD). KD rapidly reverses NAFLD and insulin resistance despite increasing circulating nonesterified fatty acids (NEFA), the main substrate for synthesis of intrahepatic triglycerides (IHTG). To explore the underlying mechanism, we quantified hepatic mitochondrial fluxes and their regulators in humans by using positional isotopomer NMR tracer analysis. Ten overweight/obese subjects received stable isotope infusions of: [D_7]glucose, [$^{13}C_4$]β-hydroxybutyrate and [3-^{13}C]lactate before and after a 6-d KD. IHTG was determined by proton magnetic resonance spectroscopy (^{1}H-MRS). The KD diet decreased IHTG by 31% in the face of a 3% decrease in body weight and decreased hepatic insulin resistance (−58%) despite an increase in NEFA concentrations (+35%). These changes were attributed to increased net hydrolysis of IHTG and partitioning of the resulting fatty acids toward ketogenesis (+232%) due to reductions in serum insulin concentrations (−53%) and hepatic citrate synthase flux (−38%), respectively. The former was attributed to decreased hepatic insulin resistance and the latter to increased hepatic mitochondrial redox state (+167%) and decreased plasma leptin (−45%) and triiodothyronine (−21%) concentrations. These data demonstrate heretofore undescribed adaptations underlying the reversal of NAFLD by KD: That is, markedly altered hepatic mitochondrial fluxes and redox state to promote ketogenesis rather than synthesis of IHTG.

carbohydrate restriction | redox | citrate synthase | insulin resistance | pyruvate carboxylase

Nonalcoholic fatty liver disease (NAFLD) is the most common chronic liver disease and can progress from steatosis to advanced liver disease, including liver cirrhosis and hepatocellular carcinoma (1–3). It is strongly associated with insulin resistance, which is characterized by excessive hepatic glucose production and compensatory hyperinsulinemia (4–10). In adipose tissue of subjects with NAFLD, insulin fails to suppress lipolysis, which leads to increased hepatic delivery of nonesterified fatty acids (NEFA), the main substrate for synthesis of intrahepatic triglycerides (IHTG) (4–11). Excess substrate and hyperinsulinemia may stimulate re-esterification and de novo lipogenesis (DNL) of fatty acids, which can further increase IHTG content and overproduction of very low-density lipoprotein (VLDL)-TG into circulation (12–16). Together, these features of NAFLD increase the risk of type 2 diabetes and cardiovascular disease (1, 2).

Since obesity is an important cause of NAFLD, its management is underpinned by weight loss (17–22). Recently, low-carbohydrate ketogenic diets (KD) have gained popularity in the treatment of obesity, type 2 diabetes, and NAFLD (23–25). While long-term data comparing different weight loss regimens in NAFLD are virtually nonexistent, a low-carbohydrate diet has been reported to induce a threefold greater IHTG loss than a low-fat, high-carbohydrate diet after 48 h of caloric restriction (26). We previously showed that a hypocaloric, KD induces an ∼30% reduction in IHTG content in 6 d despite increasing circulating NEFA (27).

While the antisteatotic effect of KD is well-established, the underlying mechanisms by which it does so remain unclear. KD increases plasma NEFA concentrations, the main substrate of IHTG (11). In the liver, NEFA can either be re-esterified into complex lipids, such as TGs, or be transported to the mitochondria to be metabolized by β-oxidation into acetyl-CoA, which in turn can either be irreversibly condensed with oxaloacetate by citrate synthase to form citrate and enter the TCA cycle for terminal oxidation to CO_2 (28, 29) or it can enter the ketogenic pathway, where it is converted into acetoacetate (AcAc) and β-hydroxybutyrate (β-OHB) (28). These mitochondrial fluxes are tightly regulated by substrate availability and product inhibition (29), mitochondrial redox state (30), and hormones, such as leptin (31) and triiodothyronine (T3) (32).

Significance

Ketogenic diet is an effective treatment for nonalcoholic fatty liver disease (NAFLD). Here, we present evidence that hepatic mitochondrial fluxes and redox state are markedly altered during ketogenic diet-induced reversal of NAFLD in humans. Ketogenic diet for 6 d markedly decreased liver fat content and hepatic insulin resistance. These changes were associated with increased net hydrolysis of liver triglycerides and decreased endogenous glucose production and serum insulin concentrations. Partitioning of fatty acids toward ketogenesis increased, which was associated with increased hepatic mitochondrial redox state and decreased hepatic citrate synthase flux. These data demonstrate heretofore undescribed adaptations underlying the reversal of NAFLD by ketogenic diet and highlight hepatic mitochondrial fluxes and redox state as potential treatment targets in NAFLD.

Author contributions: P.K.L., G.I.S., and H.Y.-J. designed research; P.K.L. recruited participants, performed clinical studies and drafted the manuscript; P.K.L., S.D., K.L., and X.-M.Z. analyzed plasma samples; A.H. and T.E.L. obtained magnetic resonance imaging data; P.K.L., S.D., K.L., X.-M.Z., A.H., T.E.L., G.W.C., K.F.P., G.I.S., and H.Y.-J. analyzed data; and P.K.L., K.F.P., G.I.S., and H.Y.-J. wrote the paper.

Reviewers: F.K., Oxford Centre for Diabetes; and R.T., Newcastle University.

The authors declare no competing interest.

[1]G.I.S. and H.Y.-J. contributed equally to this work.

[2]To whom correspondence may be addressed. Email: gerald.shulman@yale.edu or Hannele.Yki-Jarvinen@helsinki.fi.

This article contains supporting information online at https://www.pnas.org/lookup/suppl/doi:10.1073/pnas.1922344117/-/DCSupplemental.

First published March 16, 2020.

In this study we examined the effects of a short-term KD on hepatic steatosis by assessing IHTG content and liver stiffness by magnetic resonance spectroscopy/elastography (^{1}H-MRS/MRE) in 10 overweight/obese participants before and after a 6-d KD. In order to examine the effect that a short-term KD diet might have on rates of hepatic mitochondrial fat oxidation and gluconeogenesis, we applied a positional isotopomer NMR tracer analysis (PINTA) method (33–35) to assess rates of hepatic mitochondrial flux through pyruvate carboxylase (V_{PC}) relative to citrate synthase flux (V_{CS}), as well as rates of endogenous glucose, β-OHB, and lactate production by stable isotope infusions of [D_7]glucose, [$^{13}C_4$]β-OHB, and [3-^{13}C]lactate, respectively. Finally, in order to gain insights into how these hepatic mitochondrial fluxes might be regulated during a KD, we also assessed some key potential regulators of these mitochondrial fluxes (i.e., hepatic mitochondrial redox state as reflected by plasma [β-OHB]/[AcAc], plasma leptin, and T3 concentrations) in these same subjects (Fig. 1 and *SI Appendix*, Fig. S1).

Results

The Study Diet Was Ketogenic and Participants Were Compliant. Characteristics of the participants are shown in Table 1. Their dietary intakes were assessed by 3-d food records at baseline and at the end of the 6-d KD (Fig. 1*A*). Compliance was verified by measuring plasma ketone bodies (β-OHB and AcAc). Compared to the habitual diets of the participants, the study diet was very low in carbohydrates (183 ± 20 vs. 23 ± 1 g/d, before vs. after, $P < 0.000001$) (Fig. 2*A*), while intake of fat and protein remained unchanged (Fig. 2*A*). This resulted in a decrease in energy intake (2,019 ± 177 vs. 1,444 kcal/d, before vs. after, $P < 0.01$). Plasma concentrations of β-OHB increased 10-fold from 0.1 ± 0.1 to 1.0 ± 0.2 mmol/L ($P < 0.001$) (Fig. 2*B*) and AcAc 6-fold from 0.1 ± 0.1 to 0.6 ± 0.1 mmol/L ($P < 0.001$) (Fig. 2*C*). Body weight decreased on the average by 3.0 ± 0.3% from 93.5 ± 5.3 to 90.7 ± 5.2 kg ($P < 0.00001$) (Fig. 2*D* and Table 1).

KD Decreased IHTG Content. IHTG content decreased by ∼31% from 10.3 ± 2.3 to 7.1 ± 2.0% ($P < 0.001$) (Fig. 3*A*) as determined by ^{1}H-MRS. Liver stiffness as determined by MRE remained unchanged (2.6 ± 0.1 vs. 2.5 ± 0.1 kilopascals [kPa], before vs. after, $P = 0.18$) (Fig. 3*B*). Activities of plasma γ-glutamyltransferase (GGT) decreased from 48 ± 10 to 38 ± 7 U/L ($P < 0.05$) and alkaline phosphatase (ALP) from 82 ± 8 to 73 ± 7 U/L ($P < 0.05$) (Fig. 3), while plasma alanine aminotransferase (ALT) and aspartate aminotransferase (AST) remained unchanged during the diet (Table 1). The AST/ALT ratio increased significantly by ∼34% from 0.84 ± 0.09 to 1.13 ± 0.15 ($P < 0.05$) during the diet (Table 1).

KD Improved Plasma Glucose, TGs, and Insulin Sensitivity. Fasting plasma glucose concentrations decreased by 13% from 112 ± 3 to 98 ± 3 mg/dL ($P < 0.01$) (Fig. 4*A*), while fasting NEFA concentrations increased by 35% from 0.55 ± 0.02 to 0.74 ± 0.02 mmol/L ($P < 0.001$) (Fig. 4*B*). Plasma TG concentration, which in the fasting state reflects predominantly liver-derived VLDL-TGs, decreased by 25% from 1.26 ± 0.14 to 0.94 ± 0.10 mmol/L ($P < 0.01$) (Fig. 4*C*), while plasma total, LDL, or high-density lipoprotein (HDL) cholesterol concentrations remained unchanged (Table 1). The 6-d KD induced a marked improvement in insulin sensitivity, as determined from decreases in fasting serum insulin concentrations (−53%, 10.9 ± 1.8 vs. 5.1 ± 0.8 mU/L, before vs. after, $P < 0.01$) (Fig. 4*D*), C-peptide concentrations (−36%, 0.75 ± 0.07 vs. 0.48 ± 0.06 nmol/L, $P < 0.001$) (Fig. 4*E*), and homeostasis assessment of insulin resistance (HOMA-IR) (−57%, 3.0 ± 0.5 vs. 1.3 ± 0.2 AU, $P < 0.01$) (Fig. 4*F*).

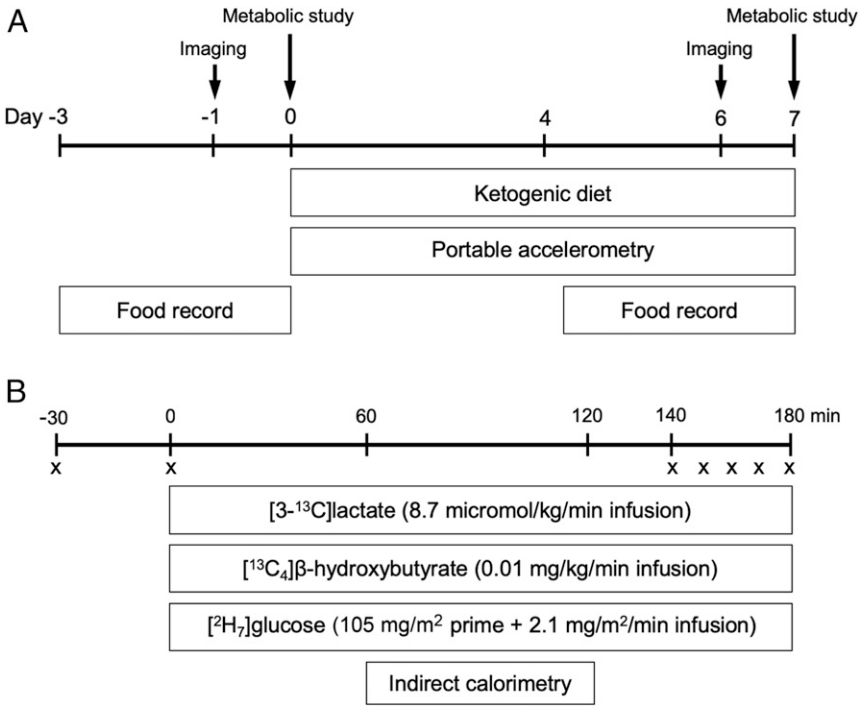

Fig. 1. Study design. (*A*) Before and after the 6-d KD, participants visited an imaging center for measurement of IHTG content and liver stiffness (days −1 and 6) and underwent metabolic studies at the Clinical Research Unit (days 0 and 7). Participants wore portable accelerometers between days 0 and 7 for determination of physical activity and recorded 3-d food intake starting at days −3 and 4 for determination of dietary composition and compliance. (*B*) During metabolic study visits, 180-min tracer infusions of lactate, β-OHB, and glucose were given for determination of rates of substrate fluxes. Indirect calorimetry was performed to measure energy expenditure and rates of substrate oxidation. An "X" denotes blood sample.

Table 1. Clinical characteristics of the participants before and after the 6-d KD

	Before	After	*P* value
Age (y)	58.2 ± 2.8	—	
Gender (*n*, women/men)	5/5	—	
Body mass index (kg/m^2)	31.6 ± 2.0	30.6 ± 2.0	<0.000001
Body weight (kg)	93.5 ± 5.3	90.7 ± 5.2	<0.00001
Fat mass (kg)	33.5 ± 4.7	32.0 ± 4.7	<0.001
Fat free mass (kg)	59.5 ± 3.8	58.5 ± 3.8	<0.01
Total body water (kg)	43.7 ± 2.8	42.7 ± 2.8	<0.001
Waist circumference (cm)	105.5 ± 4.4	102.9 ± 4.7	<0.01
Hip circumference (cm)	112.9 ± 4.3	110.3 ± 4.2	<0.001
P-ALT (IU/L)	42 ± 8	38 ± 7	0.36
P-AST (IU/L)	31 ± 3	37 ± 5	0.15
P-AST/ALT ratio	0.84 ± 0.09	1.13 ± 0.15	<0.05
P-Total cholesterol (mmol/L)	5.3 ± 0.5	5.1 ± 0.6	0.46
P-HDL cholesterol (mmol/L)	1.27 ± 0.10	1.22 ± 0.11	0.25
P-LDL cholesterol (mmol/L)	3.7 ± 0.4	3.6 ± 0.6	0.71
P-GDF15 (pg/mL)	285.9 ± 25.7	280.2 ± 27.3	0.37
P-Alanine (mmol/L)	0.32 ± 0.02	0.26 ± 0.01	0.055
Energy expenditure (kcal/24 h)	1722 ± 62	1626 ± 67	0.076
Nonprotein respiratory quotient	0.69 ± 0.02	0.65 ± 0.01	0.094
Protein oxidation (g/24 h)	72.8 ± 6.7	82.0 ± 6.1	<0.05

Data are in *n* or means ± SEM. Significances were determined by paired Student's *t* tests. GDF15, growth/differentiating factor 15; P, plasma; S, serum.

KD Altered Hepatic Mitochondrial Fluxes. The rate of endogenous glucose production decreased by 22% from 948 ± 60 to 743 ± 45 μmol/min ($P < 0.001$) (Fig. 5*A*) and the rate of endogenous lactate production decreased by 18% from 1,045 ± 83 to 860 ± 60 μmol/min ($P < 0.001$) (Fig. 5*B*) during the diet. In contrast, the rate of β-OHB production (i.e., ketogenesis) increased threefold from 174 ± 30 to 579 ± 58 μmol/min ($P < 0.001$) (Fig. 5*C*) during the diet. The ratio of the rates of hepatic V_{PC} and mitochondrial oxidation (V_{CS}) increased by 52% from 2.4 ± 0.3 to 3.6 ± 0.2 ($P < 0.001$) (Fig. 5*D*). This increase in the V_{PC}/V_{CS} ratio could entirely be attributed to a marked reduction in rates of V_{CS}, which decreased by 38% from 188 ± 20 to 116 ± 8 μmol/min ($P < 0.001$) (Fig. 5*E*), since rates of hepatic V_{PC} remained unchanged (410 ± 50 vs. 408 ± 23 μmol/min, $P = 0.97$) (Fig. 5*F*).

Potential Mechanisms Underlying the Reduction in V_{CS}. The rate of V_{CS} is highly regulated and can be inhibited by an increase in the mitochondrial redox state (29) and stimulated by hormones, such as leptin (31) and T3 (32). Hepatic mitochondrial redox state, as illustrated from an increase in the ratio of plasma β-OHB and AcAc ([β-OHB]/[AcAc]) (30, 36), increased markedly by 2.7-fold from 0.6 ± 0.1 to 1.6 ± 0.1 ($P < 0.001$) (Fig. 6*A*) during the diet. The decrease in V_{CS} was also associated with reduction in plasma concentrations of leptin by 45% from 46.5 ± 16.7 to 25.6 ± 9.5 ng/mL ($P < 0.05$) (Fig. 6*B*) and total T3 by 21% from 0.85 ± 0.08 to 0.67 ± 0.03 ng/mL ($P < 0.05$) (Fig. 6*C*).

KD Increased Protein Catabolism. Energy expenditure and nonprotein respiratory quotient remained unchanged, but rates of whole-body protein oxidation as assessed by urinary urea nitrogen excretion (37) increased by ∼13% during the diet, corresponding to an average of ∼9 g more protein being oxidized per day (Table 1).

Discussion

In the present study, we investigated the antisteatotic effects of a short-term KD by measuring IHTG content and hepatic mitochondrial fluxes by ^{1}H-MRS and PINTA. IHTG content decreased by ∼31% in 6 days (Fig. 3), whereas body weight decreased by ∼3%, and hepatic insulin resistance decreased markedly despite increases in circulating NEFA concentrations (Fig. 4), consistent with previous studies (26, 27). The decrease in IHTG content could be attributed to increased net hydrolysis of IHTG and partitioning of the resulting FA toward ketogenesis

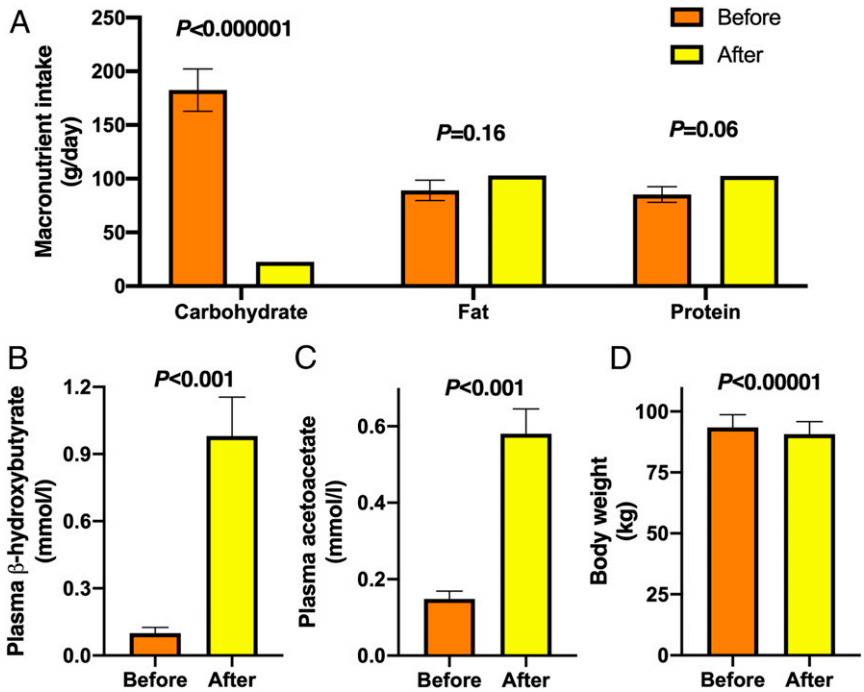

Fig. 2. The study diet was ketogenic and participants were compliant. (*A*) Macronutrient intakes, (*B*) plasma β-OHB and (*C*) plasma AcAc concentrations, and (*D*) body weight before (orange bars) and after (yellow bars) the 6-d KD ($n = 10$). Data are shown as mean ± SEM. *P* values were determined using paired Student's *t* tests.

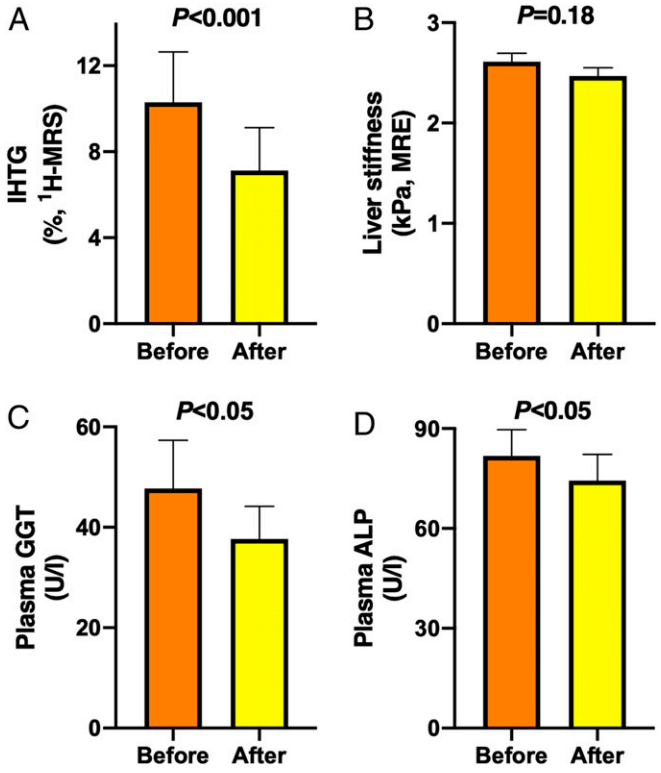

Fig. 3. KD decreased IHTG content. (*A*) IHTG content ($n = 8$), (*B*) liver stiffness ($n = 10$), (*C*) plasma GGT ($n = 10$), and (*D*) plasma ALP ($n = 9$) before (orange bars) and after (yellow bars) the 6-d KD. Data are shown as mean ± SEM. *P* values were determined using paired Student's *t* tests.

due to the accompanying reductions in serum insulin concentrations and hepatic V_{CS}, respectively (Fig. 5). Reductions in serum insulin could be attributed to decreased hepatic insulin resistance, and reductions in V_{CS} to increased hepatic mitochondrial redox state and decreased plasma leptin and T3 concentrations (Fig. 6).

The antisteatotic effect of KD is well-established, but the underlying intrahepatic adaptations are poorly understood (21, 25–27). Since better understanding of these could help to develop new approaches to treat NAFLD, we applied a PINTA method, which allows comprehensive assessment of intrahepatic mitochondrial metabolism in vivo (34). Insulin resistance is a key abnormality in NAFLD and initially is characterized by compensatory hyperinsulinemia and later by increased hepatic glucose production (5–10). In the present study, the 6-d KD markedly decreased fasting serum glucose and insulin concentrations, as well as rates of endogenous glucose production (Figs. 4 and 5), implying enhanced hepatic insulin sensitivity, consistent with previous studies (26). Rates of endogenous lactate turnover also decreased by 18% during the KD, likely reflecting decreased Cori cycling due to substrate deprivation (Fig. 5*B*) (38). Theoretically, the decrease in rates of glucose production could be due to glycogen depletion or decreased gluconeogenesis. In support of the former, KD has been shown to decrease hepatic glycogen content as measured using repeated liver biopsies in humans (39). We have previously shown that liver volume decreases by 22% during an identical 6-d KD, and that 70% of this decrease was attributed to loss of glycogen (40), similar to previous observations in 72-h fasted human individuals (41).

Oxaloacetate, a key gluconeogenic intermediate, is produced in hepatic mitochondria from glucose, lactate, and amino acids by pyruvate carboxylase (42). The rate of V_{PC} is controlled by substrate availability and allosteric activation by acetyl-CoA (42). In the present study, V_{PC} as determined by PINTA remained unchanged (Fig. 5*F*), despite decreased substrate availability (Fig. 5 *A* and *B* and Table 1), possibly due to increased allosteric activation by acetyl-CoA, as assessed by β-OHB turnover (Fig. 5*C*) (43). In addition to gluconeogenesis, oxaloacetate can be utilized in the TCA cycle, which decreased during the KD as determined by reduced V_{CS} (Fig. 5*E*) (44). Since V_{PC} remained unchanged (Fig. 5*F*), the decreased utilization of oxaloacetate in the TCA cycle implies that oxaloacetate was preferentially partitioned toward gluconeogenesis than the TCA cycle (Fig. 5*D*). Moreover, the unchanged rates of hepatic V_{PC} (Fig. 5*F*) suggest that the decreased rates of endogenous glucose production (Fig. 5*A*) was due to hepatic glycogen depletion.

Insulin resistance of white adipose tissue lipolysis is another hallmark of NAFLD (4–9). Circulating concentrations and turnover of NEFA are increased in NAFLD and the antilipolytic action of insulin is impaired (4–10). In the present study, plasma NEFA concentrations were increased (Fig. 4*B*) while IHTG content was decreased (Fig. 3*A*) during the KD, in keeping with previous studies (27). Since the antilipolytic action of insulin, as determined using a glycerol tracer combined with hyperinsulinemic-euglycemic clamp technique, increased during an identical KD diet (27), the increase in NEFA during the KD appears to be caused by reduced serum insulin concentrations rather than increased white adipose tissue insulin resistance.

One possible fate of FA in the liver is re-esterification, which is the major pathway contributing IHTG in NAFLD (11). In the present study, both IHTG content (Fig. 3*A*) and plasma TG concentrations (Fig. 4*C*) decreased markedly during the KD, consistent with previous data (27). The marked fall in IHTG is also likely to underrepresent a considerable fall in intrahepatocellular diacylglycerol content, a key mediator of hepatic insulin resistance (1, 45), under conditions of reduced net re-esterification. Insulin is a key regulator of TG metabolism in the liver and in adipose tissue, as it inhibits the hydrolysis of existing TGs and stimulates the synthesis of new TGs (14). The decrease in serum insulin, IHTG content, and fat mass, and the increase in plasma NEFA concentrations (Figs. 3 and 4 and Table 1) imply that net TG hydrolysis is accelerated by the KD diet, resulting in increased hepatic availability of FA.

An alternative hepatic fate of FA is mitochondrial β-oxidation into acetyl-CoA (28, 29). Hepatic concentrations of acetyl-CoA, as determined by β-OHB turnover (43), were increased during

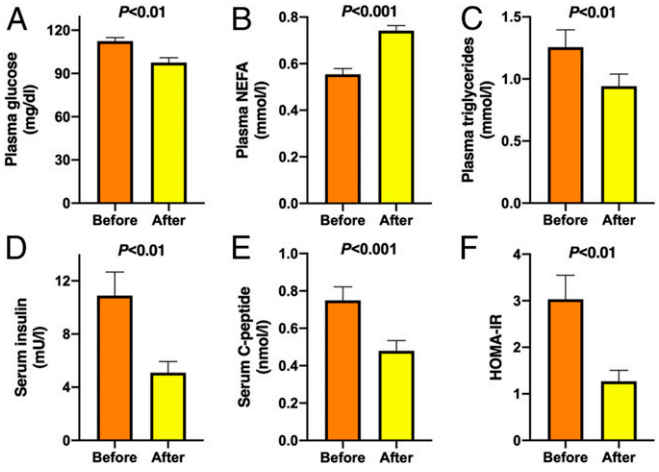

Fig. 4. KD improved plasma glucose, TGs, and insulin sensitivity. (*A*) Plasma glucose, (*B*) plasma NEFA, (*C*) plasma TG, (*D*) serum insulin, (*E*) serum C-peptide concentrations, and (*F*) HOMA-IR before (orange bars) and after (yellow bars) the 6-d KD ($n = 10$). Data are shown as mean ± SEM. *P* values were determined using paired Student's *t* tests.

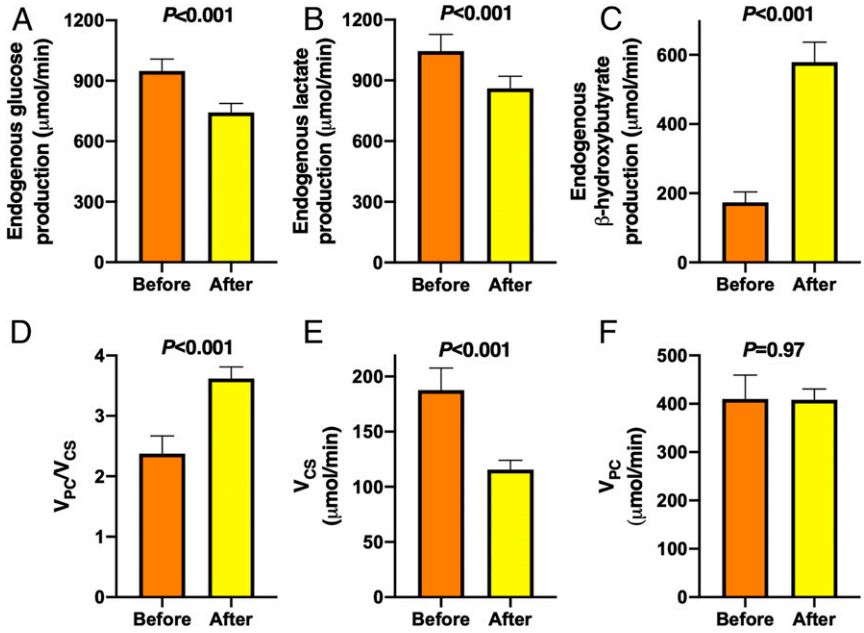

Fig. 5. KD altered hepatic mitochondrial fluxes. Rates of endogenous (*A*) glucose, (*B*) lactate, and (*C*) β-OHB production; (*D*) ratio of hepatic V_{PC} and V_{CS} fluxes, (*E*) hepatic V_{CS} flux, and (*F*) hepatic V_{PC} flux before (orange bars) and after (yellow bars) the 6-d KD ($n = 10$). Data are shown as mean ± SEM. *P* values were determined using paired Student's *t* tests.

the diet (Fig. 5*C*), suggesting that transport of FA to mitochondria and β-oxidation to acetyl-CoA was increased. Mitochondrial acetyl-CoA has two alternative metabolic fates: The oxidative pathway (i.e., the TCA cycle) and ketogenesis (28, 29). A key reaction that determines this fate is citrate synthase (46). The rate of V_{CS} flux was markedly decreased during the KD (Fig. 5*E*), which could explain why the acetyl-CoA derived by β-oxidation of FA was preferentially channeled toward ketogenesis (Fig. 5*B*) rather than the TCA cycle.

We next wished to examine the potential mechanisms underlying the reduction in V_{CS}. V_{CS} is inhibited by increased mitochondrial redox state (29). In the present study, hepatic mitochondrial redox state, as reflected by the observed increase in the [β-OHB]/[AcAc] ratio (30, 36), increased by 2.7-fold (Fig. 6*A*) during the KD. This suggests that the decrease in V_{CS} during the KD could be attributed to increased mitochondrial redox state in the liver. In addition, V_{CS} can be stimulated by hormones such as leptin (31) and T3 (32). Indeed, the decrease in V_{CS} was associated with reduced plasma concentrations of these hormones (Fig. 6 *B* and *C*), which may also have contributed to the observed reduction in V_{CS} by the KD.

Another key characteristic of NAFLD and hyperinsulinemia is increased DNL (15). We have previously shown that overfeeding of carbohydrates increases DNL and IHTG (47, 48). KD has an opposite effect (48, 49). The primary substrate in the DNL pathway is citrate, which is produced by mitochondrial citrate synthase (12). Thus, an additional contributing mechanism by which KD decreases IHTG could be a decrease in DNL due to decreases in serum insulin concentrations and V_{CS}.

Although the KD improved all metabolic abnormalities of NAFLD in just 6 d, there were also some adverse effects. The AST/ALT ratio increased by ∼34% during the diet (Table 1), suggesting that such a rapid weight loss could induce a transient hepatocellular injury, consistent with a previous study (50). In addition, the metabolic changes induced by the 6-d KD closely resembled those seen in starvation (35). Whole-body protein oxidation increased by 13% (Table 1), which in the face of unchanged dietary protein intake (Fig. 2*A*) implies that protein catabolism was increased during the KD. These data are consistent with a previous

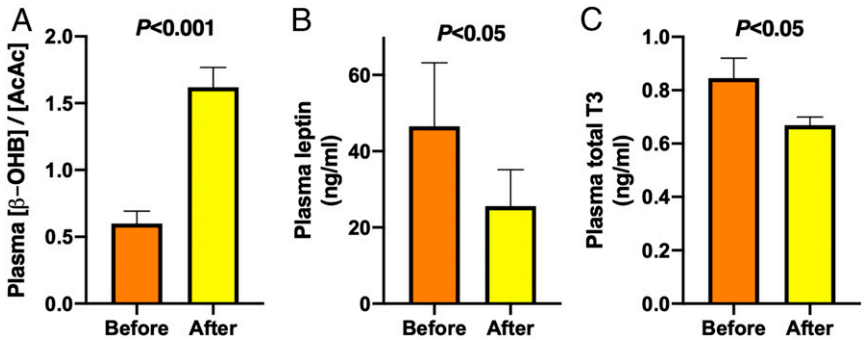

Fig. 6. Potential mechanisms underlying the reduction in V_{CS}. (*A*) Ratio of plasma β-OHB and AcAc concentrations, which reflect mitochondrial redox state, (*B*) plasma leptin concentrations, and (*C*) plasma total T3 concentrations before (orange bars) and after (yellow bars) the 6-d KD ($n = 10$). Data are shown as mean ± SEM. *P* values were determined using paired Student's *t* tests.

study showing increased urinary nitrogen excretion during KD (51), and with decreased serum concentrations of insulin (Fig. 4*D*), which stimulates protein synthesis and inhibits proteolysis in skeletal muscle (52). While the present study was designed to investigate the antisteatotic effect of short-term weight loss due to KD, it would be of interest to determine whether a more moderate, long-term and weight-stable KD has similarly beneficial effects on NAFLD and insulin sensitivity with less adverse effects as in this short-term study.

In summary, we show that a short-term (6-d) KD decreased IHTG and hepatic insulin resistance despite an increase in plasma NEFA concentrations. These changes could be attributed to increased net hydrolysis of IHTG and partitioning of the resulting FA toward ketogenesis due to reductions in serum insulin concentrations and hepatic citrate synthase flux, respectively. Taken together, these data demonstrate heretofore undescribed hepatic mitochondrial adaptations underlying the reversal of NAFLD by a short-term KD to promote ketogenesis rather than synthesis of IHTG (Fig. 7).

Materials and Methods

Participants. A total of 10 participants were recruited among individuals who had previously participated in our metabolic studies at the Clinical Research Unit (47, 53). Inclusion criteria included: 1) Age 18 to 70 y and 2) alcohol consumption <20 g/d for women and <30 g/d for men. Exclusion criteria included: 1) Known acute or chronic disease other than hepatic steatosis based on medical history, physical examination, and laboratory tests; 2) history or current use of agents associated with hepatic steatosis; 3) pregnancy or lactation; (4) intolerance to foods in the study diet; and 5) contraindications for magnetic resonance imaging (e.g., claustrophobia, metal implants). Details of the recruitment are shown in *SI Appendix*, Fig. S1 and clinical characteristics of the study subjects in Table 1. The Ethics Committee of the Hospital District of Helsinki and Uusimaa (Helsinki, Finland) approved the study protocol. The studies were performed in accordance with the Declaration of Helsinki. Each participant received an explanation of the nature and potential risks of the study prior to obtaining their written informed consent. The study was registered at ClinicalTrials.gov (NCT03737071).

Diet. The study was designed to investigate the antisteatotic effect of a 6-d KD, which we have previously shown to result in ∼3 kg weight loss and ∼30% reduction in IHTG content (27). Thus, the KD diet in the present study was similar as in the previous study and provided ∼1,440 kcal energy per day, ∼6% as carbohydrate (≤25 g/day), ∼64% as fat, and 28% as protein. All meals were prepared in the catering kitchen of the Helsinki University Hospital and provided to the participants as four frozen microwave-safe meals. The participants were contacted by phone during the intervention to ensure compliance and to address any issues. In addition, compliance was verified by 3-d food

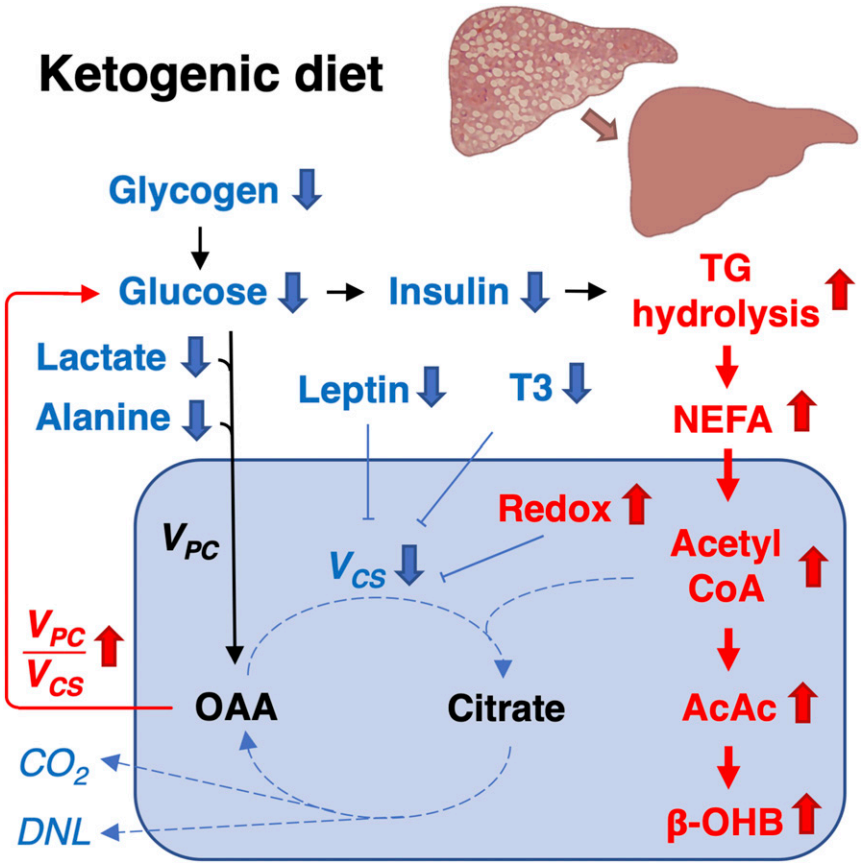

Fig. 7. Model of the antisteatotic mechanisms of KD. Glucose production decreased during the 6-d KD, which could be attributed to hepatic glycogen depletion. The decrease in glucose production was accompanied by reduced serum insulin concentrations, which promoted net hydrolysis of TGs in the liver and adipose tissue. This increased hepatic availability of fatty acids underwent β-oxidation to produce acetyl-CoA. Consequently, the hepatic mitochondrial redox state increased, which inhibited V_{CS} and diverted mitochondrial acetyl-CoA toward ketogenesis: That is, production of AcAc and β-OHB rather than into oxidation to carbon dioxide (CO_2). The reduction in V_{CS} was also associated with decreased plasma leptin and T3 concentrations. Mitochondrial V_{PC} remained unchanged during the KD, despite decreases in availability of substrates (glucose, lactate, and alanine), likely due to allosteric activation by acetyl-CoA. The increase in V_{PC}/V_{CS} diverted mitochondrial oxaloacetate (OAA) toward gluconeogenesis rather than oxidation. In addition, by limiting the availability of the primary substrate (citrate) and decreasing insulin concentrations, KD resulted in reduced hepatic DNL. Taking these data together, we find that KD improves steatosis by markedly altering hepatic mitochondrial fluxes and redox state to promote partitioning of FA to ketogenesis rather than re-esterification and lipogenesis.

records and an increase in fasting blood ketone concentrations upon admission as determined by FreeStyle Precision Neo (Abbott).

Study Design. The study consisted of 1) a screening visit, 2) visits to the imaging center for quantification of IHTG content using ^{1}H-MRS and liver stiffness using MRE, and 3) metabolic study visits (Fig. 1*A*).

Screening visit. The screening visit was performed after an overnight fast. A history and physical examination were performed to review the inclusion and exclusion criteria. Blood samples were obtained for measurement of blood count, blood hemoglobin A_{1c}, plasma glucose, creatinine, thyroid-stimulating hormone, albumin, thromboplastin time, ferritin, C-reactive protein (CRP), sodium, potassium, bilirubin, AST, ALT, ALP, GGT, serum hepatitis A and C virus, antinuclear, mitochondrial and smooth muscle antibodies, and hepatitis B surface antigen concentrations. After the screening visit, the participants were asked to collect a 3-d dietary record to determine their baseline dietary composition. The dietary records were analyzed using the AivoDiet software (v2.0.2.3; Aivo Finland, Turku, Finland).

Imaging visit. Before the metabolic study visits, the participants underwent imaging visits, which were performed after a 4-h minimum fast. IHTG content was determined by ^{1}H-MRS using Signa HDXt 1.5T scanner (GE Medical System). MR spectra were acquired using a point resolved spectroscopy sequence (TE of 30 ms, TR of 3,000 ms) and analyzed using the jMRUI v5.2 software with AMARES algorithm. Resonances of methylene groups in the FA chains and water were determined using line-shape fitting with prior knowledge. Signal intensities were corrected for T2 relaxation using the equation $I_m = I_0\exp(-TE/T2)$. T2 values of 46 ms and 58 ms were used for water and fat, respectively. IHTG content was expressed as a ratio of signal from methylene group to total signal of methylene and water, and converted from signal ratio to a weight fraction, applying method validated by Longo et al. (54) and Szczepaniak et al. (55). The following experimentally determined factors were used: 1) The ratio of the number of lipid protons in the fitted $(CH2)_{n-2}$ signal to the total number of lipid protons is 0.6332 (56); 2) proton densities of fat and water are 110 and 111 mol/l, respectively; 3) 1 g liver tissue contains 711 mg water; 4) densities of the liver tissue, fat in the liver, and water are 1.051 g/mL, 0.900 g/mL, and 1.000 g/mL; respectively. Liver stiffness was assessed using MRE (M7000MT, Resoundant Inc.). Participants were imaged lying in a supine position with an acoustic driver device on the anterior body wall overlying the liver. The acoustic driver device generated 60-Hz amplitude mechanical waves and produced shear wave motion in the abdomen. Four noncontiguous axial slices (10-mm thick, 10-mm interslice gap) were acquired through the widest transverse section of the liver. MR elastograms were generated from the wave images at the slice locations displaying stiffness in units of kilopascal. Stiffness values were calculated as a median of four consecutive measurements.

Metabolic study visit. For 3 d prior to the metabolic study day, the participants were asked to avoid foods naturally enriched in ^{13}C (such as sea food, corn, and sugar), alcohol, and strenuous physical exercise. The participants came to the clinical research center after an overnight fast. A timed urine collection was started for 260 min for determination of urinary urea excretion. Body weight was measured to the nearest 0.1 kg using a calibrated digital scale (Soehnle) with the participant wearing light indoor clothing without shoes. Height was measured to the nearest 0.5 cm using a nonstretching tape. Waist circumference was measured from the midway between the lower rib margin and the superior iliac spine, and hip circumference at the greater trochanter level. Body fat mass, fat free mass, and total body water were determined using the bioelectric impedance method (InBody 720, Biospace).

An intravenous line was inserted into an antecubital vein for infusion of the stable isotope tracers and another intravenous line was placed in a dorsal hand vein of the heated contralateral hand for sampling of "arterialized" venous blood (Fig. 1*B*). At baseline, blood samples were taken for measurement of plasma AST, ALT, ALP, GGT, CRP, LDL, and HDL cholesterol and TG, as well as serum C-peptide concentrations. Plasma β-OHB, glucose, NEFA, and serum insulin concentrations were determined at baseline and 90 and 180 min after the start of the infusions.

After the baseline blood sampling, 180-min tracer infusions of [D_7]glucose (administered as a priming dose of 105 mg/m^2 over 5 min followed by a constant infusion of 2.1 mg/m^2/min), [$^{13}C_4$]β-OHB (0.01 mg/kg/min), and [3-^{13}C] lactate (8.7 micromol/kg/min) were started (Fig. 1*B*). Arterialized plasma samples were taken at −5, 0, 140, 150, 160, 170, and 180 min for measurement of plasma enrichments of lactate, β-OHB, and glucose using GC-MS (Agilent) for determination of rates of turnover. In addition, 30 mL of plasma was collected at 180 min for analyses of positional ^{13}C isotopomer enrichments in glucose using ^{13}C MRS (Bruker Avance III HD, 500 UltraShield, TopSpin 3.2, Bruker) in combination with GC-MS and LC-MS/MS analyses, as previously described (34), for determination of hepatic rates of V_{PC} and V_{CS} fluxes.

Sixty minutes after the start of the triple tracer infusion, 40 min of indirect calorimetry was performed using a computerized flow-through canopy system (Deltatrac, Datex) to measure respiratory gas exchange and resting energy expenditure. The hood was placed over the participants' head 10 min before starting the measurements. Protein oxidation was calculated from urea concentration in urine collected for 260 min assuming that 1 mol of urea contains 28 g of urea nitrogen, and that oxidation of 6.25 g of protein produces 1 g of urea nitrogen (37). Nonprotein respiratory quotient (NPRQ) was calculated assuming that 1 g of protein requires 966 mL O_2 and produces 782 mL CO_2. Hence, $NPRQ = (VCO_2 - [782 \times P_{ox}])/(VO_2 - [966 \times P_{ox}])$, where VCO_2 is the production rate of carbon dioxide, VO_2 is the consumption rate of oxygen, and P_{ox} is protein oxidation rate in grams per minute (37). Rates of energy expenditure were calculated using the following additional assumptions: Oxidation of 1 g of carbohydrate requires 746 mL O_2 and produces 746 mL CO_2, oxidation of 1 g of lipid requires 2,029 mL of O_2 and produces 1,430 mL of CO_2, and that oxidation of 1 g carbohydrate produces 3.74 kcal, 1 g lipid 9.50 kcal, and 1 g protein 4.10 kcal (37).

At the end of the first metabolic study visit, the participants were provided with all meals of the study diet to be consumed during the 6-d dietary intervention and they were asked to collect another 3-d dietary record to determine their dietary intake during the study. The participants were also given a portable accelerometer (GT3X, Actigraph) to be worn for 6 d to measure physical activity during the 6-d KD.

The imaging and metabolic study visits were repeated with identical protocols after the 6-d KD (Fig. 1).

Laboratory Analyses. Concentrations of blood Hb_{A1c}, plasma glucose, creatinine, albumin, ferritin, CRP, sodium, potassium, bilirubin, ALT, AST, ALP, GGT, β-OHB, TGs, total cholesterol, HDL cholesterol, and serum insulin, C-peptide, hepatitis A antibody, hepatitis B surface antigen, and hepatitis C antibody were determined using Architect C16000 autoanalyzer (Abbott) (57). Blood counts were assessed by impedance, flow cytometric, and photometric assay (XN10, Sysmex). Plasma thyroid-stimulating hormone concentration was assessed using Architect i2000SR autoanalyzer (Abbott). Plasma thromboplastin time was determined using the Owren method by Nycotest PT (Axis Shield). Serum antinuclear, antimitochondrial, and antismooth muscle antibodies were assessed using indirect immunofluorescence assays. Plasma growth/differentiating factor 15 (GDF15) concentration was determined using GDF15 DuoSet ELISA kit (R&D Systems). Plasma AcAc concentration was determined by a colorimetric assay (Biovision). Plasma leptin and T3 concentrations were assessed using double antibody radio-immunoassays (Linco). Plasma NEFA concentrations were measured using enzymatic, colorimetric assay (Wako Diagnostics). Plasma alanine concentrations were measured by GC-MS after spiking the samples with a ^{2}H-alanine internal standard and comparing the ratio of labeled to unlabeled substrate to a standard curve. Urinary urea was determined by photometric, enzymatic assay using Architect C16000 (Abbott). Concentrations of glucose and lactate infusates were assessed by YSI 2700 analyzer (YSI Inc), and those of β-OHB were determined by COBAS MIRA Plus (Roche). HOMA-IR was calculated using the formula: HOMA-IR = fS-insulin (mU/l) × fP-glucose (mg/dL)/405.

Calculations. Rates of [D_7]glucose, [$^{13}C_4$]β-OHB and [3-^{13}C]lactate turnover were calculated during isotopic steady state as the tracer infusion rate × [(infusate enrichment/plasma enrichment) − 1]. V_{PC}/V_{EGP} and V_{PC}/V_{CS} were calculated from the ^{13}C glucose enrichments: m+1, m+2, [4-^{13}C]glucose, [5-^{13}C]glucose, as previously derived (34, 35).

Statistics. Continuous variables were tested for normality using the Shapiro–Wilk test. Nonnormally distributed data were log-transformed for analysis and back-transformed for presentation. The paired Student's *t* test was used to compare data at the end of the study to the baseline. Data were reported in means ± SE of means. Statistical analyses were using GraphPad Prism 8.1.2 for Mac OS X (GraphPad Software). A *P* value of less than 0.05 indicated statistical significance.

Material and Data Availability. Sources for materials used in this study are described in *Materials and Methods*. The raw data obtained for this study are presented in Dataset S1.

ACKNOWLEDGMENTS. The authors thank Aila Rissanen for advice in diet design; Aila Karioja-Kallio, Päivi Ihamuotila, and Kimmo Porthan for their excellent clinical assistance; Gina Butrico, Irina Smolgovsky, John Stack, Maria Batsu, Codruta Todeasa, and the Yale Hospital Research Unit for excellent technical assistance; Anni Honkala, Niina Laihanen, Maria Riihelä, Maria

Rautamo, and Kaisa Jousimies for assistance with infusates; Titta Kaukinen and Jussi Perkiö for assistance with imaging; Heini Oksala and Karri Mikkonen for assistance with diets; Siiri Luukkonen for graphical assistance; and the volunteers for their help. This study was supported by Academy of Finland Grant 309263 (to H.Y.-J.); EU H2020 project 'Elucidating Pathways of Steatohepatitis' EPoS Grant 634413 (to H.Y.-J.); and H2020-JTI-IMI2 EU project 777377-2 Liver Investigation: Testing Marker Utility in Steatohepatitis (LITMUS) (to H.Y.-J.), Erityisvaltionosuus (H.Y.-J.); Sigrid Jusélius Foundation (H.Y.-J., P.K.L.); Finnish Diabetes Research Foundation (P.K.L.); Instrumentarium Foundation (P.K.L.); Novo Nordisk (P.K.L.) Foundation; and the United States Public Health Service Grants R01 DK113984 (to G.I.S.), P30 DK45735 (to G.I.S.), and UL1 RR024139 (to Yale Hospital Research Unit).

1. V. T. Samuel, G. I. Shulman, Nonalcoholic fatty liver disease as a nexus of metabolic and hepatic diseases. *Cell Metab.* **27**, 22–41 (2018).
2. H. Yki-Järvinen, Non-alcoholic fatty liver disease as a cause and a consequence of metabolic syndrome. *Lancet Diabetes Endocrinol.* **2**, 901–910 (2014).
3. J. C. Cohen, J. D. Horton, H. H. Hobbs, Human fatty liver disease: Old questions and new insights. *Science* **332**, 1519–1523 (2011).
4. E. Fabbrini *et al*., Alterations in adipose tissue and hepatic lipid kinetics in obese men and women with nonalcoholic fatty liver disease. *Gastroenterology* **134**, 424–431 (2008).
5. A. Gastaldelli *et al*., Relationship between hepatic/visceral fat and hepatic insulin resistance in nondiabetic and type 2 diabetic subjects. *Gastroenterology* **133**, 496–506 (2007).
6. K. M. Korenblat, E. Fabbrini, B. S. Mohammed, S. Klein, Liver, muscle, and adipose tissue insulin action is directly related to intrahepatic triglyceride content in obese subjects. *Gastroenterology* **134**, 1369–1375 (2008).
7. A. Kotronen, L. Juurinen, M. Tiikkainen, S. Vehkavaara, H. Yki-Järvinen, Increased liver fat, impaired insulin clearance, and hepatic and adipose tissue insulin resistance in type 2 diabetes. *Gastroenterology* **135**, 122–130 (2008).
8. E. Bugianesi *et al*., Insulin resistance in non-diabetic patients with non-alcoholic fatty liver disease: Sites and mechanisms. *Diabetologia* **48**, 634–642 (2005).
9. A. Seppälä-Lindroos *et al*., Fat accumulation in the liver is associated with defects in insulin suppression of glucose production and serum free fatty acids independent of obesity in normal men. *J. Clin. Endocrinol. Metab.* **87**, 3023–3028 (2002).
10. L. Ryysy *et al*., Hepatic fat content and insulin action on free fatty acids and glucose metabolism rather than insulin absorption are associated with insulin requirements during insulin therapy in type 2 diabetic patients. *Diabetes* **49**, 749–758 (2000).
11. K. L. Donnelly *et al*., Sources of fatty acids stored in liver and secreted via lipoproteins in patients with nonalcoholic fatty liver disease. *J. Clin. Invest.* **115**, 1343–1351 (2005).
12. M. K. Hellerstein, J. M. Schwarz, R. A. Neese, Regulation of hepatic de novo lipogenesis in humans. *Annu. Rev. Nutr.* **16**, 523–557 (1996).
13. D. F. Vatner *et al*., Insulin-independent regulation of hepatic triglyceride synthesis by fatty acids. *Proc. Natl. Acad. Sci. U.S.A.* **112**, 1143–1148 (2015).
14. R. Zechner *et al*., FAT SIGNALSLipases and lipolysis in lipid metabolism and signaling. *Cell Metab.* **15**, 279–291 (2012).
15. J. E. Lambert, M. A. Ramos-Roman, J. D. Browning, E. J. Parks, Increased de novo lipogenesis is a distinct characteristic of individuals with nonalcoholic fatty liver disease. *Gastroenterology* **146**, 726–735 (2014).
16. M. Adiels *et al*., Overproduction of large VLDL particles is driven by increased liver fat content in man. *Diabetologia* **49**, 755–765 (2006).
17. K. F. Petersen *et al*., Reversal of nonalcoholic hepatic steatosis, hepatic insulin resistance, and hyperglycemia by moderate weight reduction in patients with type 2 diabetes. *Diabetes* **54**, 603–608 (2005).
18. European Association for the Study of the Liver (EASL); European Association for the Study of Diabetes (EASD); European Association for the Study of Obesity (EASO), EASL-EASD-EASO Clinical Practice Guidelines for the management of non-alcoholic fatty liver disease. *J. Hepatol.* **64**, 1388–1402 (2016).
19. M. Tiikkainen *et al*., Effects of identical weight loss on body composition and features of insulin resistance in obese women with high and low liver fat content. *Diabetes* **52**, 701–707 (2003).
20. E. Vilar-Gomez *et al*., Weight loss through lifestyle modification significantly reduces features of nonalcoholic steatohepatitis. *Gastroenterology* **149**, 367–378.e365, quiz e314–365 (2015).
21. J. D. Browning, J. Davis, M. H. Saboorian, S. C. Burgess, A low-carbohydrate diet rapidly and dramatically reduces intrahepatic triglyceride content. *Hepatology* **44**, 487–488 (2006).
22. E. L. Lim *et al*., Reversal of type 2 diabetes: Normalisation of beta cell function in association with decreased pancreas and liver triacylglycerol. *Diabetologia* **54**, 2506–2514 (2011).
23. J. Abbasi, Interest in the ketogenic diet grows for weight loss and type 2 diabetes. *JAMA* **319**, 215–217 (2018).
24. G. D. Foster *et al*., A randomized trial of a low-carbohydrate diet for obesity. *N. Engl. J. Med.* **348**, 2082–2090 (2003).
25. C. Thoma, C. P. Day, M. I. Trenell, Lifestyle interventions for the treatment of non-alcoholic fatty liver disease in adults: A systematic review. *J. Hepatol.* **56**, 255–266 (2012).
26. E. Kirk *et al*., Dietary fat and carbohydrates differentially alter insulin sensitivity during caloric restriction. *Gastroenterology* **136**, 1552–1560 (2009).
27. K. Sevastianova *et al*., Genetic variation in PNPLA3 (adiponutrin) confers sensitivity to weight loss-induced decrease in liver fat in humans. *Am. J. Clin. Nutr.* **94**, 104–111 (2011).
28. J. D. McGarry, D. W. Foster, Regulation of hepatic fatty acid oxidation and ketone body production. *Annu. Rev. Biochem.* **49**, 395–420 (1980).
29. H. A. Krebs, Rate control of the tricarboxylic acid cycle. *Adv. Enzyme Regul.* **8**, 335–353 (1970).
30. H. A. Krebs, T. Gascoyne, The redox state of the nicotinamide-adenine dinucleotides in rat liver homogenates. *Biochem. J.* **108**, 513–520 (1968).
31. R. B. Ceddia *et al*., Leptin stimulates uncoupling protein-2 mRNA expression and Krebs cycle activity and inhibits lipid synthesis in isolated rat white adipocytes. *Eur. J. Biochem.* **267**, 5952–5958 (2000).
32. M. B. Weinberg, M. F. Utter, Effect of thyroid hormone on the turnover of rat liver pyruvate carboxylase and pyruvate dehydrogenase. *J. Biol. Chem.* **254**, 9492–9499 (1979).
33. L. Goedeke *et al*., Controlled-release mitochondrial protonophore (CRMP) reverses dyslipidemia and hepatic steatosis in dysmetabolic nonhuman primates. *Sci. Transl. Med.* **11**, eaay0284 (2019).
34. R. J. Perry *et al*., Non-invasive assessment of hepatic mitochondrial metabolism by positional isotopomer NMR tracer analysis (PINTA). *Nat. Commun.* **8**, 798 (2017).
35. K. F. Petersen, S. Dufour, G. W. Cline, G. I. Shulman, Regulation of hepatic mitochondrial oxidation by glucose-alanine cycling during starvation in humans. *J. Clin. Invest.* **129**, 4671–4675 (2019).
36. D. H. Williamson, P. Lund, H. A. Krebs, The redox state of free nicotinamide-adenine dinucleotide in the cytoplasm and mitochondria of rat liver. *Biochem. J.* **103**, 514–527 (1967).
37. E. Ferrannini, The theoretical bases of indirect calorimetry: A review. *Metabolism* **37**, 287–301 (1988).
38. A. Freminet, C. Poyart, L. Leclerc, M. Gentil, Effect of fasting on the Cori cycle in rats. *FEBS Lett.* **66**, 328–331 (1976).
39. L. H. Nilsson, E. Hultman, Liver glycogen in man—The effect of total starvation or a carbohydrate-poor diet followed by carbohydrate refeeding. *Scand. J. Clin. Lab. Invest.* **32**, 325–330 (1973).
40. H. Bian, A. Hakkarainen, N. Lundbom, H. Yki-Järvinen, Effects of dietary interventions on liver volume in humans. *Obesity (Silver Spring)* **22**, 989–995 (2014).
41. D. L. Rothman, I. Magnusson, L. D. Katz, R. G. Shulman, G. I. Shulman, Quantitation of hepatic glycogenolysis and gluconeogenesis in fasting humans with 13C NMR. *Science* **254**, 573–576 (1991).
42. J. R. Williamson, E. T. Browning, M. Olson, Interrelations between fatty acid oxidation and the control of gluconeogenesis in perfused rat liver. *Adv. Enzyme Regul.* **6**, 67–100 (1968).
43. R. J. Perry, L. Peng, G. W. Cline, K. F. Petersen, G. I. Shulman, A non-invasive method to assess hepatic acetyl-CoA in vivo. *Cell Metab.* **25**, 749–756 (2017).
44. O. E. Owen, S. C. Kalhan, R. W. Hanson, The key role of anaplerosis and cataplerosis for citric acid cycle function. *J. Biol. Chem.* **277**, 30409–30412 (2002).
45. M. C. Petersen, G. I. Shulman, Roles of diacylglycerols and ceramides in hepatic insulin resistance. *Trends Pharmacol. Sci.* **38**, 649–665 (2017).
46. O. Wieland, L. Weiss, I. Eger-Neufeldt, Enzymatic regulation of liver acetyl-CoA metabolism in relation to ketogenesis. *Adv. Enzyme Regul.* **2**, 85–99 (1964).
47. P. K. Luukkonen *et al*., Saturated fat is more metabolically harmful for the human liver than unsaturated fat or simple sugars. *Diabetes Care* **41**, 1732–1739 (2018).
48. K. Sevastianova *et al*., Effect of short-term carbohydrate overfeeding and long-term weight loss on liver fat in overweight humans. *Am. J. Clin. Nutr.* **96**, 727–734 (2012).
49. A. Mardinoglu *et al*., An integrated understanding of the rapid metabolic benefits of a carbohydrate-restricted diet on hepatic steatosis in humans. *Cell Metab.* **27**, 559–571.e5 (2018).
50. H. E. Johansson *et al*., Energy restriction in obese women suggest linear reduction of hepatic fat content and time-dependent metabolic improvements. *Nutr. Diabetes* **9**, 34 (2019).
51. P. H. Bisschop *et al*., Dietary carbohydrate deprivation increases 24-hour nitrogen excretion without affecting postabsorptive hepatic or whole body protein metabolism in healthy men. *J. Clin. Endocrinol. Metab.* **88**, 3801–3805 (2003).
52. T. Pozefsky, P. Felig, J. D. Tobin, J. S. Soeldner, G. F. Cahill, Jr, Amino acid balance across tissues of the forearm in postabsorptive man. Effects of insulin at two dose levels. *J. Clin. Invest.* **48**, 2273–2282 (1969).
53. P. K. Luukkonen *et al*., Human PNPLA3-I148M variant increases hepatic retention of polyunsaturated fatty acids. *JCI Insight* **4**, 127902 (2019).
54. R. Longo *et al*., Proton MR spectroscopy in quantitative in vivo determination of fat content in human liver steatosis. *J. Magn. Reson. Imaging* **5**, 281–285 (1995).
55. L. S. Szczepaniak *et al*., Magnetic resonance spectroscopy to measure hepatic triglyceride content: Prevalence of hepatic steatosis in the general population. *Am. J. Physiol. Endocrinol. Metab.* **288**, E462–E468 (2005).
56. L. S. Szczepaniak *et al*., Measurement of intracellular triglyceride stores by H spectroscopy: Validation in vivo. *Am. J. Physiol.* **276**, E977–E989 (1999).
57. S. Lallukka *et al*., Predictors of liver fat and stiffness in non-alcoholic fatty liver disease (NAFLD) - an 11-year prospective study. *Sci. Rep.* **7**, 14561 (2017).